JOURNAL OF GEOPHYSICAL RESEARCH, VOL. 105, NO. D8, PAGES 10,129–10,146, APRIL 27, 2000

Space-time rainfall organization and its role in validating quantitative precipitation forecasts

Jesus Zepeda-Arce and Efi Foufoula-Georgiou

St. Anthony Falls Laboratory, Department of Civil Engineering, University of Minnesota, Minneapolis

Kelvin K. Droegemeier

Center for Analysis and Prediction of Storms and School of Meteorology, University of Oklahoma, Norman

Abstract. The scope of this paper is to introduce a suite of new multiscale statistical measures which can be used, in addition to traditional measures, to compare observed and model-predicted patterns for model validation. Recent research on analysis of observed precipitation patterns at a multitude of scales has revealed interesting spatial and spatiotemporal organizations which have often been related to physical properties of the storm environment. By testing whether this multiscale statistical organization is also reproduced in the model-predicted patterns or whether there are significant biases and disagreements in such comparisons is conjectured to hold promise for understanding model performance and guiding future model improvements. Results from application of the developed methodologies to the May 7-8, 1995, multisquall line storm over central Oklahoma are presented and discussed in light of the additional information gained by the new validation measures as compared to traditional measures.

1. Introduction

Accurate forecasting of the onset, duration, motion, location, and intensity of precipitation is one of the most difficult challenges facing modern-day meteorology. The economic and societal impacts of such forecasts are enormous, ranging from the mitigation of life and property loss associated with flash floods to the application of effective management strategies in hydroelectric power generation. The next quantum leap in quantitative precipitation forecasting (QPF) is the explicit representation of storm-scale features in non-hydrostatic numerical models; thus increasing attention is now being given to storm-scale predictability [e.g., *Droegemeier* 1997].

An important initial step toward improving storm-scale QPF involves establishing and correcting deficiencies in current microphysical parameterization schemes through realistic simulation experiments using high-quality observations (e.g., the Next Generation Radar (NEXRAD) products) for both input and verification. Procedures for effectively using these data as input and in an assimilation mode are already well explored [e.g., see *Droegemeier et al.*, 1996a, b; *Xue et al.*, 1996a, b]. However, methods that compare forecasted high-resolution precipitation patterns to observed ones at a range of scales such that deficiencies in microphysical parameterizations and other small-scale structure representations can be depicted lag behind. Traditional measures of forecast performance [e.g., see *Mesinger*, 1996; *Murphy and Winkler*, 1987] are too coarse for this purpose. They provide valuable information on the model's ability to reproduce the areal extent and total precipitation amounts but only limited information about the model's ability to mimic the statistical-dynamical environment that created the observed spatiotemporal rainfall pattern. Consequently, there is limited feedback for model improvement.

In this paper, we propose some new statistical measures which can depict how well the multiscale spatial structure and space-time dynamics of forecasted precipitation fields match those of the observed fields. We demonstrate through a case study that these new measures contain additional information not available from traditional measures. We advocate that the proposed methodologies, if used in conjunction with the existing ones, may improve our understanding of model performance and provide a systematic way of assessing and guiding future model improvements in terms of improved microphysics, increased model resolution and improved data assimilation.

Throughout this paper, the term "domain" is used to denote the areal extent of an analyzed field. The term "resolution" is used to denote the smallest grid size at which observations or model outputs of a field are avail-

Paper number 1999JD901087.
0148-0227/00/1999JD901087$09.00

able. The term "scale" is used to denote any grid size at which one chooses to view the field. In this paper, only scales larger than the resolution of the original field (i.e., not subgrid scales) are used, and the values of the field at those scales are obtained from the original field via averaging. Section 2 presents the theory behind the proposed measures. Section 3 implements these measures in a case study, the storm of May 7-8, 1995, over central Oklahoma and discusses the results. Conclusions and directions for future research are presented in section 4.

2. Proposed Multiscale Statistical Measures for Assessing Forecast Performance

2.1. Threat Score as a Function of Scale

The threat score (TS) measures the ability in correctly predicting the area of the storm having precipitation amounts exceeding a given threshold [e.g., see *Wilks*, 1995; *Fritsch et al.*, 1998]. It is defined as TS $= A_c/(A_o + A_f - A_c)$, where A_c is the correctly forecast area bounded by a given precipitation amount, A_o is the observed area and A_f is the forecast area.

It should be noted that the computed value of TS carries with it a specific "scale" at which the observed or forecast pattern is seen. Usually, this scale is the "resolution" of the numerical model but does not necessarily have to be so. One could envision situations where a storm-scale model is run at high resolution (e.g., 1 or 3 km grid size), whereas the assessment of the forecast is needed at a larger scale pertinent to a hydrologic application, for example, a scale below which rainfall variability has been found not to affect the predicted runoff for a basin or even the scale of the whole basin if a lumped hydrologic model is to be used. Obviously, as the scale increases the prediction (as judged by the TS) becomes better. The rate of TS improvement as a function of scale can be seen as an extension of the typical TS measure and can provide additional information for model verification as demonstrated in section 3.

2.2. Depth-Area-Duration Curves

For a fixed duration, the depth-area (DA) curve is a plot of rainfall depth versus the area of the storm over which that depth is exceeded. Depth-area-duration (DAD) curves are extensively used in hydrologic modeling to reconstruct precipitation patterns and provide them as input to rainfall/runoff models for computation of design hydrographs. A DAD curve does not directly compare the observed and predicted precipitation patterns in terms of their overlapping areas but rather depicts the areally variable internal structure of precipitation patterns irrespective of their location. Such a measure ignores differences arising from incorrect prediction of the location of the storm and instead concentrates on comparing the internal spatial structure of the predicted and observed precipitation patterns. The same is true for the other two measures discussed in sections 2.3 and 2.4.

2.3. Scale-to-Scale Spatial Variability and Scaling

The structure of rainfall variability as a function of scale has been studied by many researchers over the past decade [e.g., see *Schertzer and Lovejoy* [1987], *Gupta and Waymire* [1990], *Kumar and Foufoula-Georgiou* [1993a, b], *Olsson et al.* [1993], *Tessier et al.* [1993], *Harris et al.* [1996], *Over and Gupta* [1996], *Veneziano et al.* [1996], among others). These studies have demonstrated the presence of an interesting scale-invariant structure in the organization of spatial precipitation fields and have explored it for process understanding, relation of statistical to physical descriptions, and development of efficient stochastic rainfall models and rainfall downscaling schemes.

An extensive study of several warm-season convective storms in the midwestern United States by *Perica and Foufoula-Georgiou* [1996a] revealed that standardized spatial rainfall fluctuations, defined as $\xi_L = X_L'/\overline{X_L}$, where X_L' is the spatial fluctuation (difference of intensities in adjacent pixels) and $\overline{X_L}$ is the local rainfall average at scale L, exhibit Gaussianity and simple scaling over at least the range of 4–64 km scales. This implies that the variance of fluctuations at one scale relates to that at another scale via the ratio of the two scales and not their absolute values, i.e.,

$$\sigma_{\xi,L_1}/\sigma_{\xi,L_2} = (L_1/L_2)^H . \qquad (1)$$

In other words, the increase of variance with scale remains constant in a logarithmic scale, i.e., $\log \sigma_{\xi,L}$ versus $\log L$ plots as a straight line with slope H. This scale-independent constant value of H reflects how the variance is distributed within a precipitation system from larger to smaller scales. In the case that a pronounced directionality is present in the storm system, fluctuations in the latitudinal ($i = 1$), longitudinal ($i = 2$), and diagonal directions ($i = 3$) are considered separately, and three scaling parameters $\{H_i\}_{i=1,2,3}$ are computed.

It was found empirically by analysis of several midlatitude convective storms that the parameter H (or average of H_1, H_2, and H_3 in the case of pronounced directionality) is related to the convective available potential energy (CAPE) in the prestorm environment (*Perica and Foufoula-Georgiou*, [1996b]) as

$$H = 0.0516 + 0.9646(\mathrm{CAPE} \times 10^{-4}), \qquad (2)$$

where CAPE is given in $\mathrm{m^2\ s^{-2}}$. Notice that this predictive relationship implies that the higher the value of CAPE, the larger the value of H and thus the higher the growth of variability of normalized rainfall fluctuations as a function of scale.

If such a spatial organization and scale invariance is found to exist in the observed precipitation patterns, one wonders whether this structure is also found to exist in patterns predicted by atmospheric models. If yes, this could provide more confidence that the model physics and spatial resolution correctly capture the observed storm dynamics. If not, it could provide useful feedback for model improvements, especially in physical parameterizations. It is stressed that other measures of multiscale rainfall variability than the one used here could be employed. For example, one could use the structure of the break-down coefficients [e.g., *Harris et al.*, 1996], the parameters of a multiplicative cascade model [e.g., *Over and Gupta*, 1996], or the parameters of a universal cascade [e.g., *Schertzer and Lovejoy*, 1987]. Also, the presence of scale invariance is not a requirement for the use of multiscale statistical measures for model verification. Scale invariance provides a convenient and parsimonious representation, for example, a single parameter H in our case. However, the whole log σ_ξ versus log L curve could have been used as a measure if approximation by a straight line was not possible.

It is interesting to note that the proposed measure for multiscale comparison of normalized rainfall fluctuations (or gradients) can be seen as an extension of the traditional $S1$ score. The $S1$ score which was introduced in the 1950s [e.g., *Teweles and Wobus*, 1954] compares horizontal gradients of the predicted and observed fields but only at one scale, typically the spacing of the grid. One of its limitations as discussed by *Wilks* [1995] was exactly this scale dependency. The proposed multiscale measure nicely overcomes this limitation by comparing gradients at a multitude of scales. Moreover, owing to the resulting scale-invariant parameterization, which was possible by working with the normalized rainfall gradients and not with the gradients themselves as the $S1$ score does, the proposed measure is very parsimonious.

2.4. Spatiotemporal Organization

As in any evolving natural process, including precipitation, variability in space and time are related to each other in ways that are not obvious by direct observation of the complex spatiotemporal patterns. Recently, *Venugopal et al.* [1999a, b] demonstrated that there exists a simple scale-invariant spatiotemporal organization in rainfall patterns which can be unraveled by proper renormalization of the space and time coordinates.

Let $I^L_{i,j}(\tau)$ and $I^L_{i,j}(\tau + t)$ represent rainfall intensity values averaged over a box of size L centered around spatial location (i, j) of the precipitation field at two instants of time τ and $\tau + t$, respectively. The evolution of the field at scale L and a time period t was characterized by *Venugopal et al.* [1999a] by differences in the logs of the rainfall intensities $\Delta \ln I$, i.e.,

$$\Delta \ln I_{i,j,\tau}(L,t) = \ln(I^L_{i,j}(\tau + t)) - \ln(I^L_{i,j}(\tau)). \quad (3)$$

This selection was made since there is evidence that the temporal fluctuations of the rainfall process linearly depend on the background rainfall intensities and thus the normalized fluctuations (by the background intensity) or the differences in the logs of intensities are independent identically distributed random variables [see *Venugopal et al.*, 1999a].

The $\Delta \ln I$ measure described above was evaluated for all locations (i, j) and all time instants τ, and for various spatial and temporal scales, L and t, respectively. Then assuming stationarity in space (i.e., independence of the specific (i, j) position) and selecting regions in time where the statistics (mean and variance) of $\Delta \ln I$ do not significantly deviate from their average value for that region, the probability density functions (pdfs) of $\Delta \ln I(L, t)$ were formed for various spatial and temporal scales, L and t, respectively.

Venugopal [1999] and *Venugopal et al.* [1999a] found, by analysis of several storms in different geographical regions of the world (the tropical region of Darwin, Australia, the forested region of BOREAS in northern Saskatchewan, and the Oklahoma region in the midwestern United States) that the pdf of $\Delta \ln I(L, t)$ remains statistically invariant if space and time are renormalized with the transformation $t/L^z = \text{constant}$. That is, the evolution of the rainfall field at spatial scale L_1 and during a time lag t_1 is statistically identical to the evolution of the rainfall field at spatial scale L_2 and time lag t_2, as long as

$$t_1/t_2 = (L_1/L_2)^z, \quad (4)$$

where z is the so-called dynamic scaling exponent. If such organization is found in the observed space-time patterns of a specific storm, it is relevant to determine whether the model-produced patterns respect the same spatiotemporal organization and if not, how to interpret the differences.

3. Results From a Case Study

3.1. Predicted and Observed Rainfall Patterns

The storm-scale weather prediction model adopted for this study was the Advanced Regional Prediction System (ARPS), developed at the Center for Analysis and Prediction of Storms (CAPS) at the University of Oklahoma [*Xue et al.*, 1995]. ARPS is a three-dimensional, nonhydrostatic numerical prediction system which includes a data ingest, quality control and objective analysis package known as ARPS Data Analysis System (ADAS) [*Brewster*, 1996], a single-Doppler radar parameter retrieval and assimilation system known as ARPS Data Assimilation System (ARPS-DAS), of which ADAS is a component, the ARPS prediction model itself, and postprocessing packages known as ARPSPLT and ARPSVIEW. The ARPS model was selected for its advanced abilities, good documentation and flexibility of operation on broad classes of comput-

ers. Nonetheless, the measures defined in this paper and the results obtained are of general interest and not particular to a specific model.

We selected as a case study the multiple squall line storm system of May 7-8, 1995. The synoptic conditions of this storm, radar observations, and the details of the numerical experiments are given by *Wang et al.* [1996] and *Shapiro et al.* [1996]. The ARPS model was used in a one-way nested mode. The outer, coarse-grid domain was 4032 × 4032 km (18-km grid spacing), and the inner grid domain was 1008 × 1008 km (6-km grid spacing). Fifty-three levels were used in the vertical, and the vertical grid spacing varied from 20 m near the ground to 980 m at the model top. There were 21 grid levels in the lowest 2 km.

Identical model physics were used on the coarse and fine grids except for moist processes. The coarse grid included grid-scale condensation only, while the Kessler warm-rain microphysics scheme was used on the fine grid. A 1.5-order of Turbulent Kinetic Energy (TKE)-based subgrid scale turbulence and a soil model coupled with surface energy budget equations and an atmospheric radiation package were used.

Starting at 1200 UTC on May 7, 1995, the model was run at the coarse grid domain for 18 hours with the Rapid Update Cycle (RUC) analysis as the background field [e.g., see *Benjamin et al.*, 1994]. The lateral boundaries were forced by linearly interpolating the 6-hour RUC forecasts that started at 1200 UTC. Using the ADAS analysis at 1800 UTC, the 6-hour forecasts on the 18-km grid were used as the background and Oklahoma Mesonet and Weather Surveillance Doppler Radar (WSR-88D) data were assimilated in a new analysis. The surface and near-surface fields were most impacted by the addition of the Mesonet surface observations.

We used the model-predicted precipitation fields in the inner grid domain (resolution of 6 km). The simulation started at 1200 UTC (denoted as $t = 0$ hours of the simulation time) on May 7, 1995. Data assimilation included hourly nonradar data (surface observations from the Oklahoma Mesonet) from 1200 to 1700 UTC and Level II radial velocity data every 15 min from 1700 to 1800 UTC. The simulation ended at 0600 UTC, May 8, 1995 (denoted as $t = 18$ hours of the simulation). For this storm, radar-converted rainfall accumulations were available every hour, and both radar reflectivities and radar-converted rainfall intensities were available every 6 min [see *Zepeda-Arce*, 1999]. The Z-R relationship used to convert reflectivities to rainfall intensities is $Z = 300.86R^{1.40}$. This relationship was calibrated using raingauge observations and was found appropriate for the Twin Lakes radar [e.g., see *Smith et al.*, 1996]. It is worth noting that the scaling parameters H and z are not overly sensitive to uncertainties in the Z-R relationship (e.g., see sensitivity analysis by *Perica and Foufoula-Georgiou* [1996a]), and this gives confidence that estimates of these parameters depict the multiscale statistical structure of the storms and are not artifacts of our assumptions.

The domains over which the observed and model-predicted precipitation fields were available together with the spatial and temporal resolutions of the fields are summarized in Table 1 and displayed in Figure 1. As can be seen from this table, the domains over which the predicted fields were available are much larger than the domains over which observations were available. In order to meaningfully compare the statistics of the ob-

Table 1. Domains and Resolutions Used for the Comparison of Observed and Model-Predicted Patterns of the May 7-8, 1995, Storm

Field	Time Resolution	Space Resolution, km^2	Largest Domain Available, km^2	Domain Used for Scaling Analysis, km^2	Number of Pixels of Domain Used in Scaling Analysis	Domain Used for TS and DAD Comparison, km^2
Observed	1 hour	4 × 4	768 × 768	512 × 512 (R1)	128 × 128	768 × 768
Predicted	1 hour	6 × 6	1008 × 1008	768 × 768 (M1)	128 × 128	768 × 768
Observed	18-min	4 × 4	304 × 304	304 × 304 (R2)	76 × 76	—
Predicted	15-min	6 × 6	1008 × 1008	768 × 768 (M2)	128 × 128	—

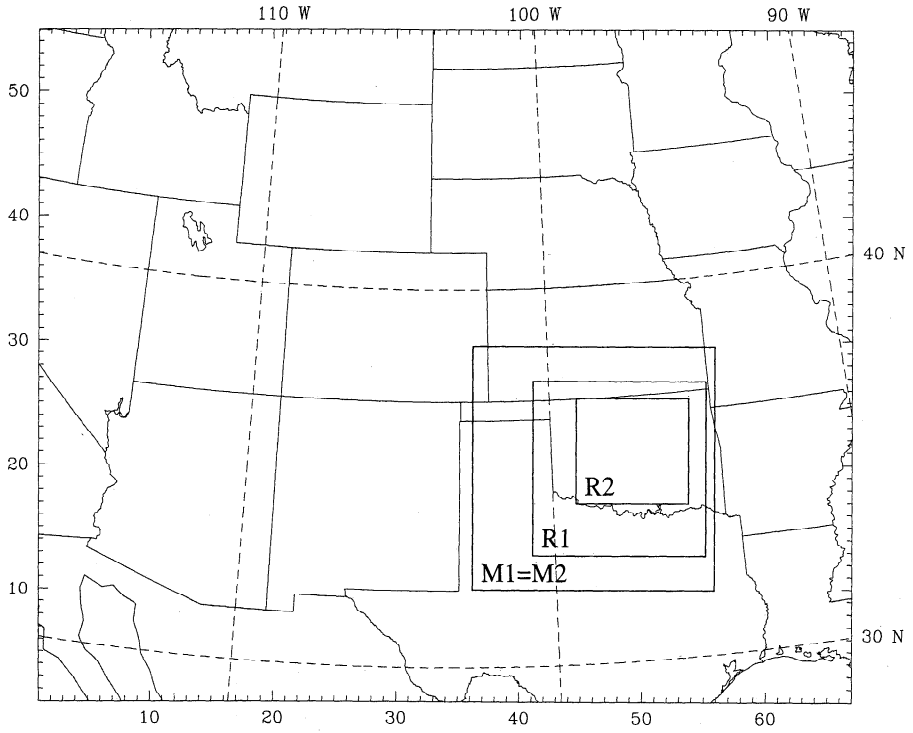

Figure 1. Domains over which the predicted and observed precipitation fields were analyzed: R1, domain of 1-hour observed rainfall accumulations; R2, domain of 18-min observed rainfall accumulations; M1 and M2, domain of 1-hour and 15-min predicted rainfall accumulations (see Table 1).

served and predicted fields, (colocated) subdomains of comparable size were selected for the analysis.

For comparison of the threat score (TS) and the depth-area-duration (DAD) curves of the 1-hour rainfall accumulations, a domain of 768 × 768 km^2 for both model and observations was chosen. The scaling analysis requires dyadic scales which implies that the domain size must be equal to the resolution times an integer power of 2. This constrains the domains to be of size $4 \times 2^7 = 512$ km for the observed fields and $6 \times 2^7 = 768$ km for the modeled fields. For the 18-min observed fields, a padding of zeros was used to extend the domain of 304 × 304 km^2 to the required size of 512 × 512 km^2. This padding was done at the top left corner of the domain and was checked that it did not affect the results of the scaling analysis.

As can be seen from Figure 2, at around 2200 UTC (t = 10 hours of simulation) of May 7 a second squall line started entering the simulation domain. This new squall line stayed in the domain until the end of the simulation period while the original squall line moved out of the domain at around 0100 UTC (t = 13 hours of simulation) of May 8 (see Figure 2). During the transition period (t = 11–13 hours of simulation), the statistical structure of the precipitation field within the domain of observation was different than before or after the transition as will be discussed later in section 3.3.

Figure 3 shows the model-predicted 1-hour accumulated fields. At t = 9 and 10 hours of the simulation, the predicted storm is more scattered than the observed storm. After that it organizes in a squall line until the end of the storm. The predicted amounts are much greater than the observed amounts throughout the simulation as can be seen from the maxima hourly accumulations reported in Figures 2 and 3. This is an issue that needs careful investigation but is beyond the scope of the present article. It is emphasized that all our measures (except the DAD curves) are normalized measures, and thus they compare the similarity of the statistical structure of the fields irrespectively of discrepancies in their absolute magnitudes.

3.2. Threat Score and Depth-Area-Duration Curves

The TS and DAD curves were computed for the hourly observed and model-predicted accumulated patterns throughout the storm evolution. Here only the results after the transition period, i.e., for t = 13–15 hours of the simulation are presented and discussed. This is because during that period the second squall line was well established in both the observed and model-predicted systems and comparison with storm-depth dependent measures (such as TS and the DAD curve) would be more meaningful.

The TS was computed at the scale of 12 km (common scale between the radar data available at 4 km resolution and model data available at 6 km resolution). A threshold depth of 5 mm accumulation in 1 hour was

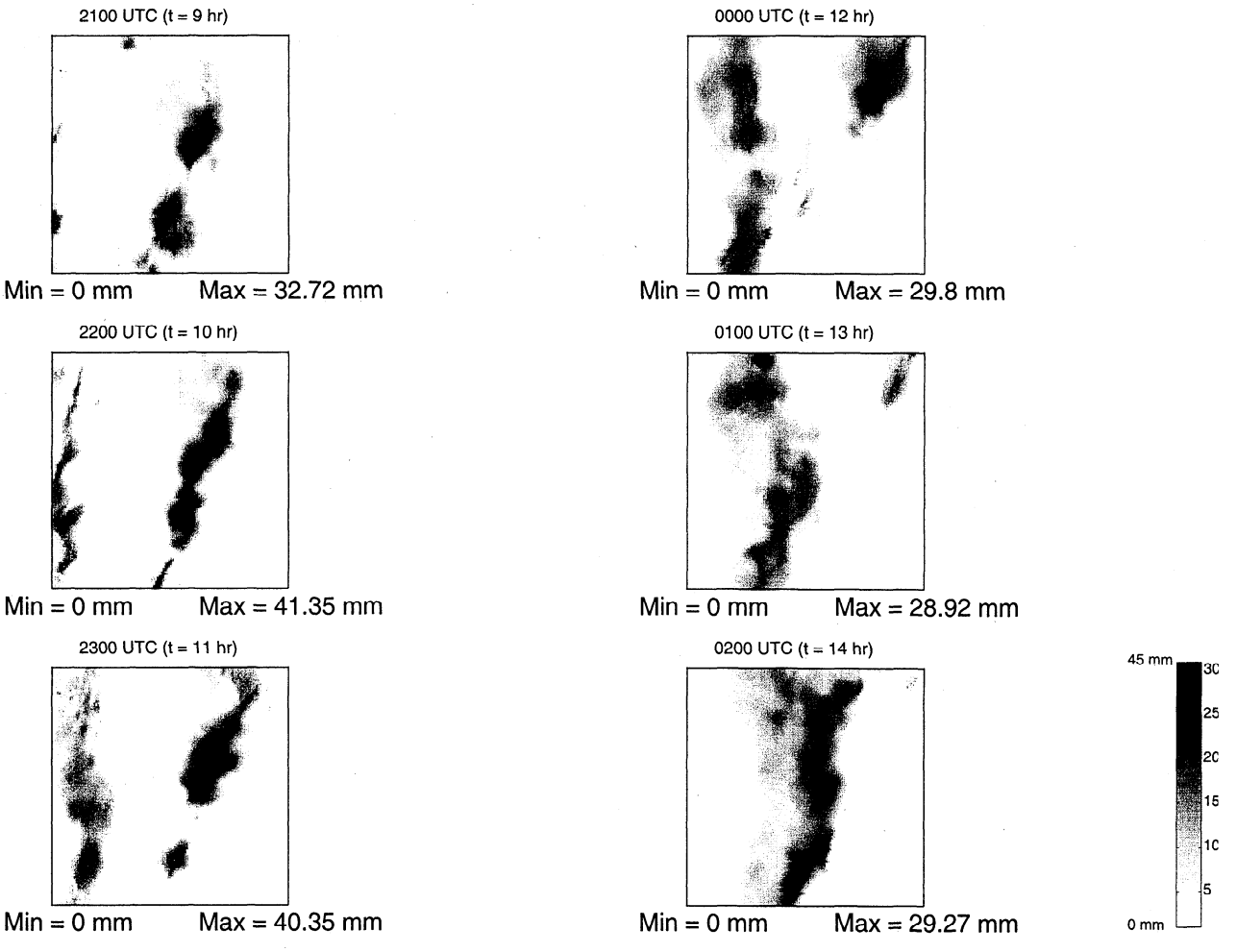

Figure 2. One-hour radar rainfall accumulations of the May 7-8, 1995, storm at resolution of 4 km. The square box has dimensions 512 × 512 km^2. Note that the scale we used for the display of magnitudes is normalized such that the range of rainfall accumulations (maximum-minimum) is mapped logarithmically onto 30 gray shades. The panels shown are for 2100, 2200, and 2300 UTC on May 7, 1995, and 0000, 0100, and 0200 UTC on May 8, 1995.

used to classify a pixel as rainy or dry. It is interesting to observe from Figure 4 that in all cases the TS value at scale of 12 km is almost zero, indicating that the forecast and observed patterns had very little (if any) overlap. As we change the scale at which the patterns are compared, the TS increases (see Figure 4, left). At $t = 13$, even at scales as large as 768 km, the TS is very low (value of 0.2), whereas at $t = 14$ and $t = 15$ hours at such large scales the TS is perfect (value of 1.0). This indicates that the model has better captured the location of the pattern at $t = 14$ and 15 hours compared to t = 13 hours. This is also depicted in Figure 5a, which displays the TS versus scale curves as the storm evolved. Judging from the values of TS at the small scale of 12 km, this forecast would not be judged very successful. Even more important, little feedback for improving the model has really resulted from this measure. The rate of TS change with scale provided more information indicating a constant improvement of model performance over time, and this is consistent with the results found from the DAD curves discussed next.

The DAD curves of the predicted and observed 1-hour accumulation patterns at $t = 13$, 14, and 15 hours are shown in Figures 4 (right). At $t = 13$ hours and $t = 14$ hours, the model DAD curves are far from those of the observations. This implies that the model-predicted depths are much higher for a given areal coverage or alternatively that for a given depth, a much lesser area with this or greater amount was predicted than actually occurred. However, at $t = 15$ hours the DAD curve reflects a drastic change of the model forecast ability. The model and observed curves are very close to each other, while the TS has remained the same and has not reflected this improvement. It is interesting also to notice that the tendency of the DAD curves with time in the model was in the opposite direction from that

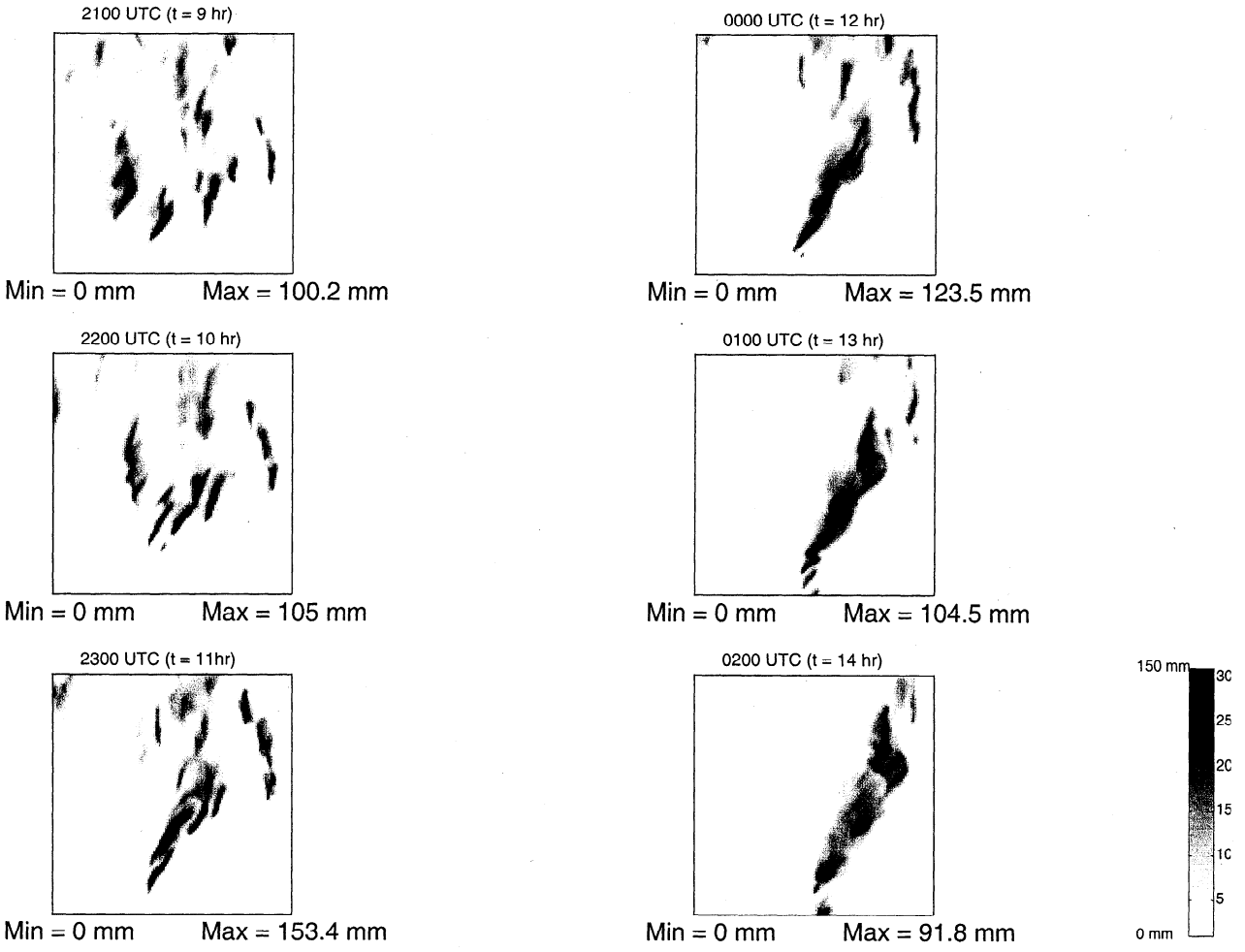

Figure 3. One-hour model-predicted rainfall accumulations of the May 7-8, 1995, storm at resolution of 6 km. The square box has dimensions of 768 × 768 km^2. Note that the scale we used for the display of magnitudes is normalized such that the range of accumulations (maximum-minimum) is mapped logarithmically on the 30 gray shades. The panels shown are for 2100, 2200, and 2300 UTC on May 7, 1995, and 0000, 0100, and 0200 UTC of May 8, 1995.

of the observed patterns (see Figure 5b). During the 3 hours ($t = 13-15$ hours), the DAD curves of the model-predicted patterns decreased while of the observed patterns increased. Obviously, this tendency is related to the build-up or dissipation of the storm which might not be well reproduced in the model for this particular case. Analysis of more storms needs to be performed to better understand this measure and its significance in suggesting model improvements.

3.3. Spatial Scale-to-Scale Variability

3.3.1. One-hour radar-observed versus model-predicted accumulations. The 1-hour radar-observed accumulated precipitation patterns were analyzed at different scales, and the scale-to-scale variability of the standardized rainfall fluctuations was computed as discussed in section 2.3. Figure 6 shows, as an example, the standard deviations of the normalized rainfall fluctuations with scale for the three directional components (latitudinal, longitudinal, and diagonal) at one instant of time ($t = 12$ hours) for the radar-observed and model-predicted fields. Similar plots were found for all other hours. A good log-log linear relationship in the standard deviation of normalized spatial fluctuations with scale, as evidenced by a high R value, implies the presence of simple scaling.

It was found that all values of R were above 0.96 (and most of them were even above 0.98) implying good scaling throughout the storm for both the observed and model-predicted hourly accumulated patterns. Occasionally, the model-predicted patterns showed a slight tendency of concavity in the log-log plots. This resulted in slightly lower R values although all above 0.96 implying still a good approximation to scaling. Only for $t = 14$ hours, the standard deviation of the normalized fluctuations of the model-predicted patterns at the largest scale of 96 km was too low and was not included in the estimation of the H values.

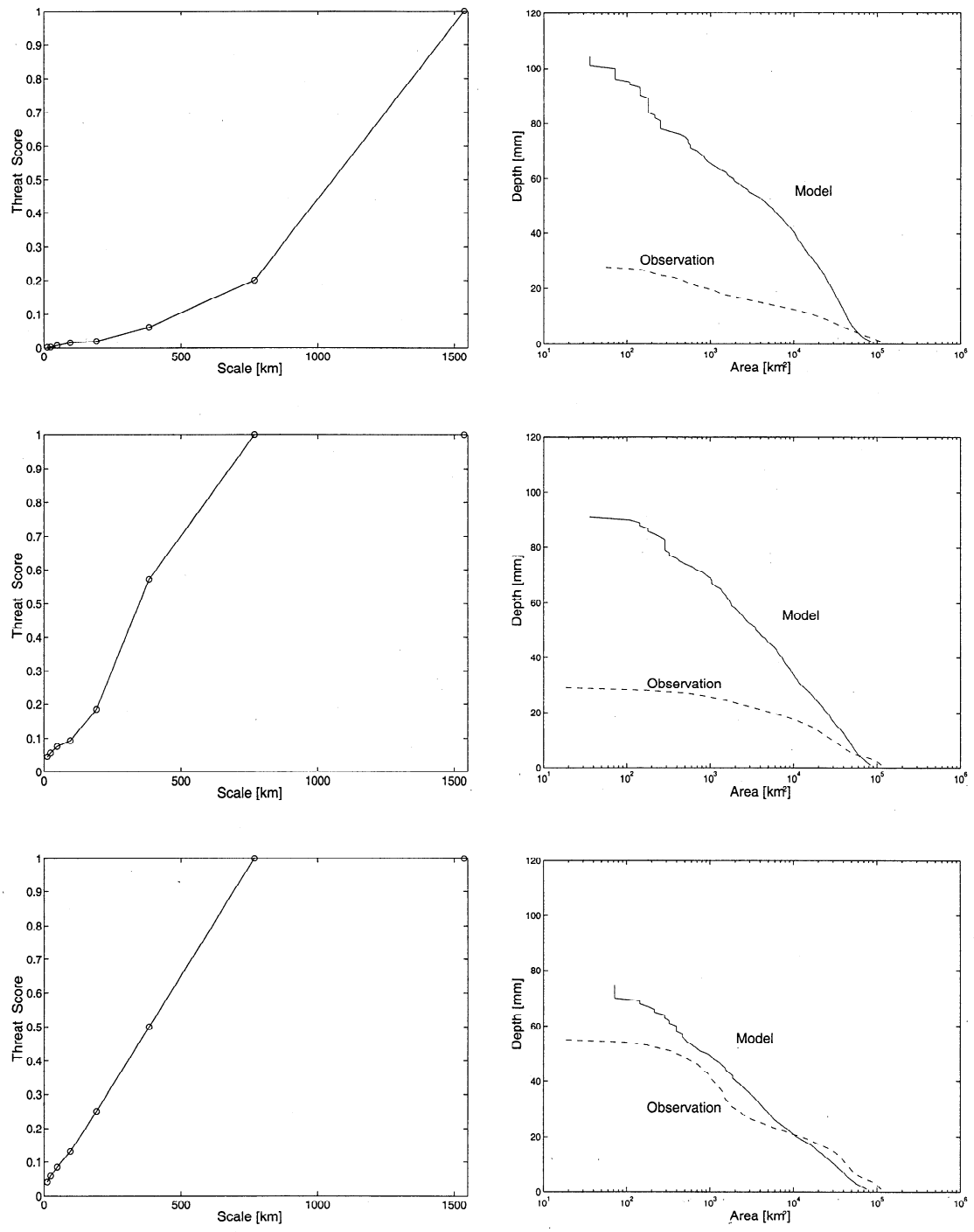

Figure 4. The left plots display the TS as a function of scale, and the right plots show the depth-area curves for the observed and predicted 1-hour accumulation patterns. The plots shown above are for (top) $t = 13$, (middle) $t = 14$, and (bottom) $t = 15$ hours of the simulation.

The values of the estimated parameters H_1, H_2, and H_3 as a function of time for the observed and model-predicted patterns are shown in Figures 7a and 7b, respectively. Comparison of Figures 7a and 7b reveal some subtle differences between the variability of the normalized spatial fluctuations in the observed and model-predicted patterns. First, the values of H in the observed patterns show a more pronounced change over time than in the model. This change is associated with the transition period during which the original squall line moved out of the domain (between $t = 11$ and 13 hours) and the new squall line was established (after $t = 13$ hours). This new squall line had generally larger values of H than the original squall line. In addition, it was observed that throughout the storm the values of H_1 and H_2 of the model were lower than H_1 and

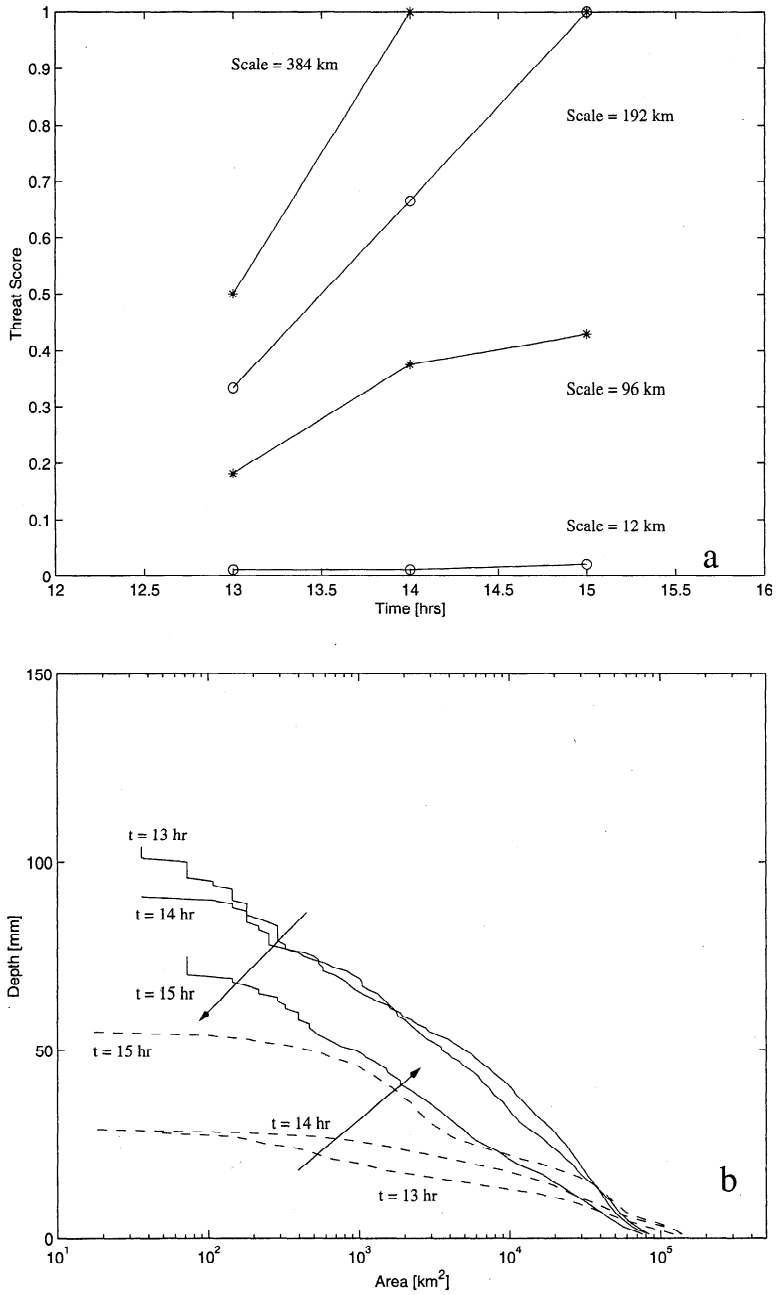

Figure 5. (top) The comparison of the threat score as a function of scale for the period t = 13-t = 15 hours of the simulation. (bottom) The DAD curves for t = 13, 14, and 15 hours computed from the model-predicted (solid lines) and radar-observed (broken lines) 1-hour accumulation patterns.

H_2 of observations and that the difference between the diagonal component H_3 and the other two components was larger in the model than in the observations. It is noted that although generally $H_{\text{model}} < H_{\text{obs}}$, the standard deviations of the normalized fluctuations in all directions were almost always higher in the model than in the observations, i.e., $\sigma_{\xi,\text{model}} > \sigma_{\xi,\text{obs}}$ (e.g., see Figure 6).

These findings indicate that the model-predicted normalized fluctuations are in general more variable than the observed. However, the growth of this variability with scale is slower in the model than in the observations at least for the longitudinal and latitudinal components. In the diagonal direction, the scale-to-scale variability growth in the model is comparable to that of the observations. Further research will test whether increasing the resolution of the model (reduction to grid size of 1 km or less) will produce a better agreement between the scaling statistical features of the observed and predicted fields.

3.3.2. Eighteen-minute radar-observed and fifteen-min model-predicted accumulations. Sin-

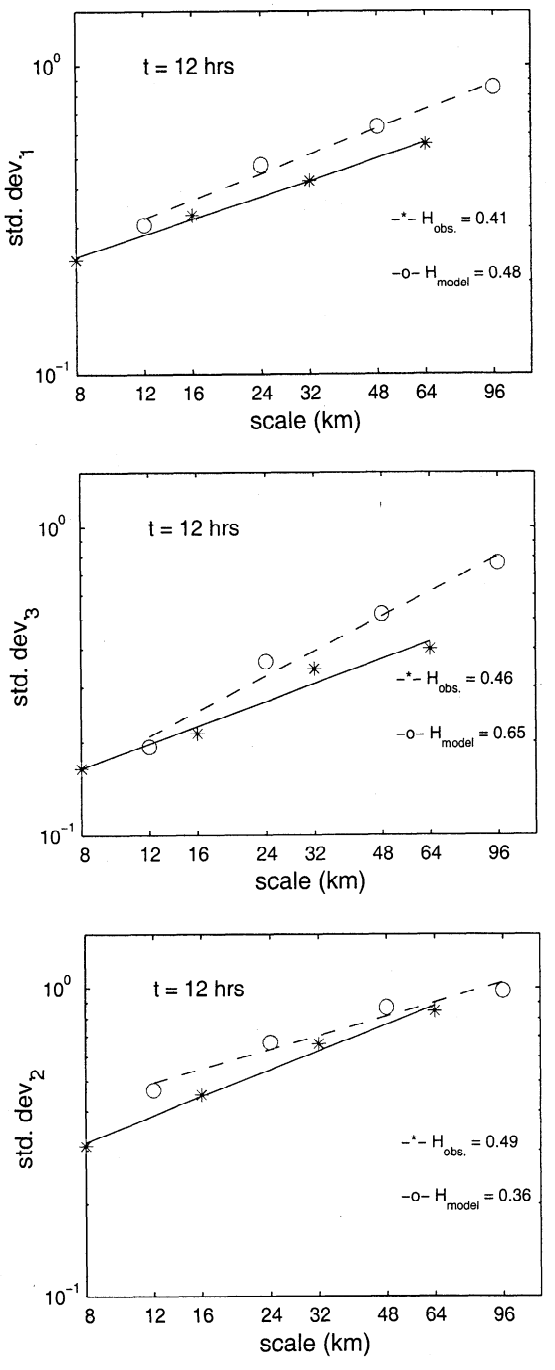

Figure 6. Log-log plots of the standard deviations of the normalized spatial rainfall fluctuations (in the latitudinal, longitudinal, and diagonal direction) versus scale for the 1-hour rainfall accumulations from the radar-observed (stars with solid lines) and model-predicted (circles with fitted broken lines) at 0000 UTC ($t = 12$ hours) on May 8 1995. Log-log linearity suggests presence of simple scaling.

ce 1-hour rainfall accumulations integrate out the fine-scale rainfall variability (i.e., that caused by small-scale convection), the scaling analysis was also applied to finer temporal scale rainfall accumulations: 18-min accumulations for the observed radar patterns and 15-min accumulations for the predicted patterns. A sample of the log-log plots of the standard deviation of latitudinal fluctuations with scale for these patterns is shown in Figure 8. Similar plots were found for the other components. Log-log plots with $R \geq 0.95$ were considered as a good approximation to scaling. For the diagonal fluctuations, whose interpretation is second derivatives [see *Perica and Foufoula-Georgiou*, 1996b], the requirement for scaling was relaxed to $R \geq 0.90$ since there is greater uncertainty in estimating the values of the diagonal fluctuations.

Figures 9a and 9b summarize the results of the analysis. When scaling was not present (as judged by the above criteria) the estimated values of H are reported, but the lack of scaling is marked on the plot by a dark square. As can be seen from Figures 9, the comparison of the 18-min and 15-min rainfall accumulations is more revealing than the comparison of the hourly accumulations. Generally, the model was not able to reproduce the pronounced temporal variation of H_1, H_2, and H_3 during the storm evolution. It is interesting to observe that the change in the storm's statistical structure during ($t = 11-13$ hours) and after the transition period ($t > 13$ hours) is well captured by the scale-to-scale variability parameter H in the observations: During the transition a break in scaling was found, and after the transition (when the new squall line was established within the domain) the parameters H increased significantly. No such change was observed in the model-produced patterns which had an almost constant to only slightly increasing values of H during that period. No directionality seemed to be present in the observed patterns and $H_1 \simeq H_2 \simeq H_3$. However, the diagonal component (H_3) was significantly higher than H_1 and H_2 (by approximately 0.2) in the model. Again, as in the hourly accumulations, the standard deviations of the normalized fluctuations in the latitudinal, longitudinal, and diagonal directions in the model, $\sigma_{\xi,\text{model}}$ were higher than $\sigma_{\xi,\text{obs}}$ at any scale and at all times (e.g., see Figure 8). Further investigation is needed to conclude whether the difference between the statistical multiscale structure of the observed and modeled patterns has physical significance and what this can imply for adjusting the model physics to better reproduce the observed patterns.

3.3.3. Six-minute radar-observed rainfall accumulations. Finally, the scaling analysis was also applied to the 6-min accumulations of the radar-observed patterns. This was done in order to (1) understand the multiscale statistical structure of the observed fields at the finest temporal resolution available and (2) get a better idea of the effects of temporal averaging on the results of the scaling analysis. The results of this analysis are summarized in Figure 10. All points at which scaling was not a good approximation (using again the criteria of $R \geq 0.95$ for H_1 and H_2 and $R \geq 0.90$ for H_3) are marked with a dark square on Figure 10.

As is observed from Figure 10, the latitudinal and longitudinal components of the standardized rainfall fluc-

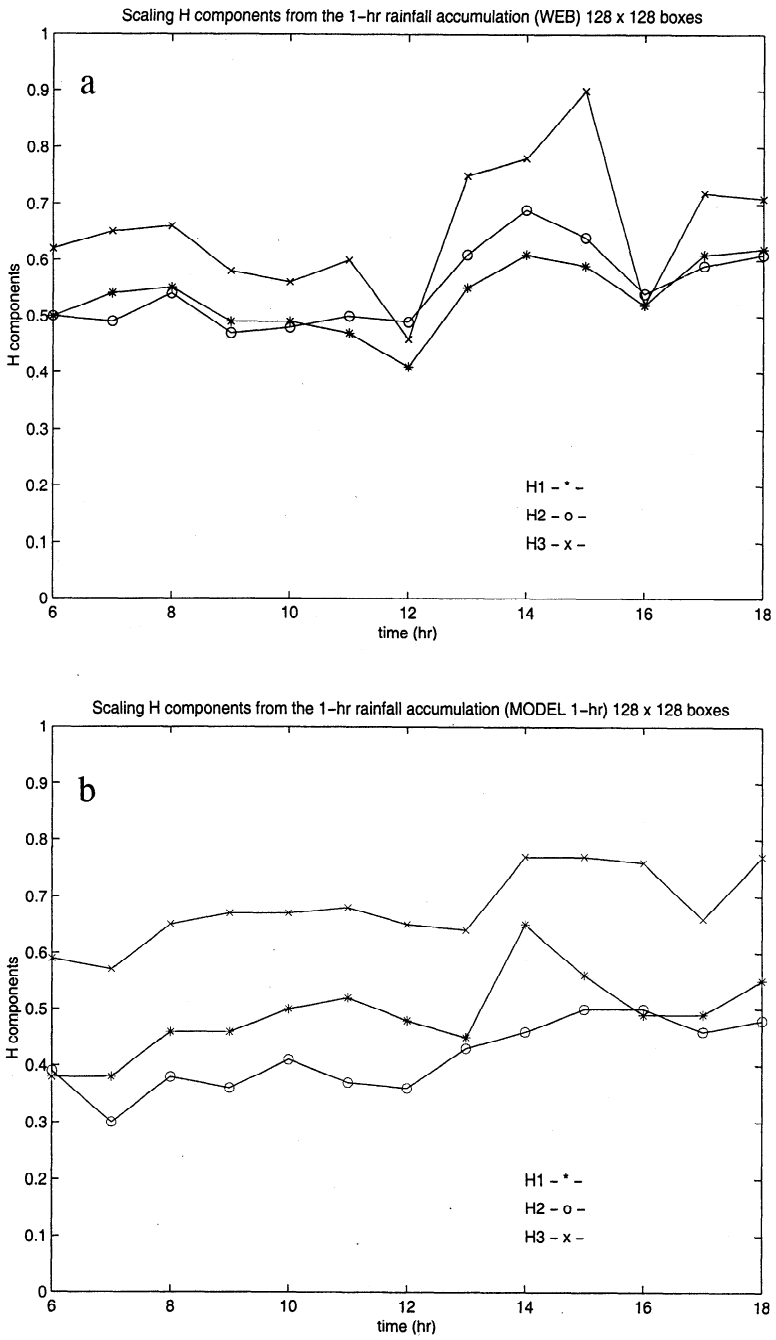

Figure 7. Scaling parameters H_1, H_2, H_3 versus time from the (a) 1-hour observed and (b) 1-hour predicted accumulated precipitation fields.

tuations exhibited good scaling throughout the storm except during the transition period of $t = 11-13$ hours. This agrees with the conclusions reached by the analysis of the 18-min rainfall accumulations. Before and after the transition period (i.e., when each of the squall lines was fully established within the domain), scaling was present in the longitudinal and latitudinal components but not in the diagonal component. As discussed earlier, the diagonal component of fluctuations is equivalent to a second-order gradient (see explanation given by *Perica and Foufoula-Georgiou*, [1996a]) which has greater uncertainty in its computation especially at larger scales. Break of scaling in the diagonal component was also found from the 18-min observed accumulations but not from the 15-min model-predicted accumulations.

Comparison of Figure 10 with Figure 9a reveals that the multiscale statistical structure of the 6-min rainfall accumulations is similar to that of the 18-min accumulations in terms of the values of the estimated parameters H and their temporal variation over the storm duration. This suggests that the pronounced temporal

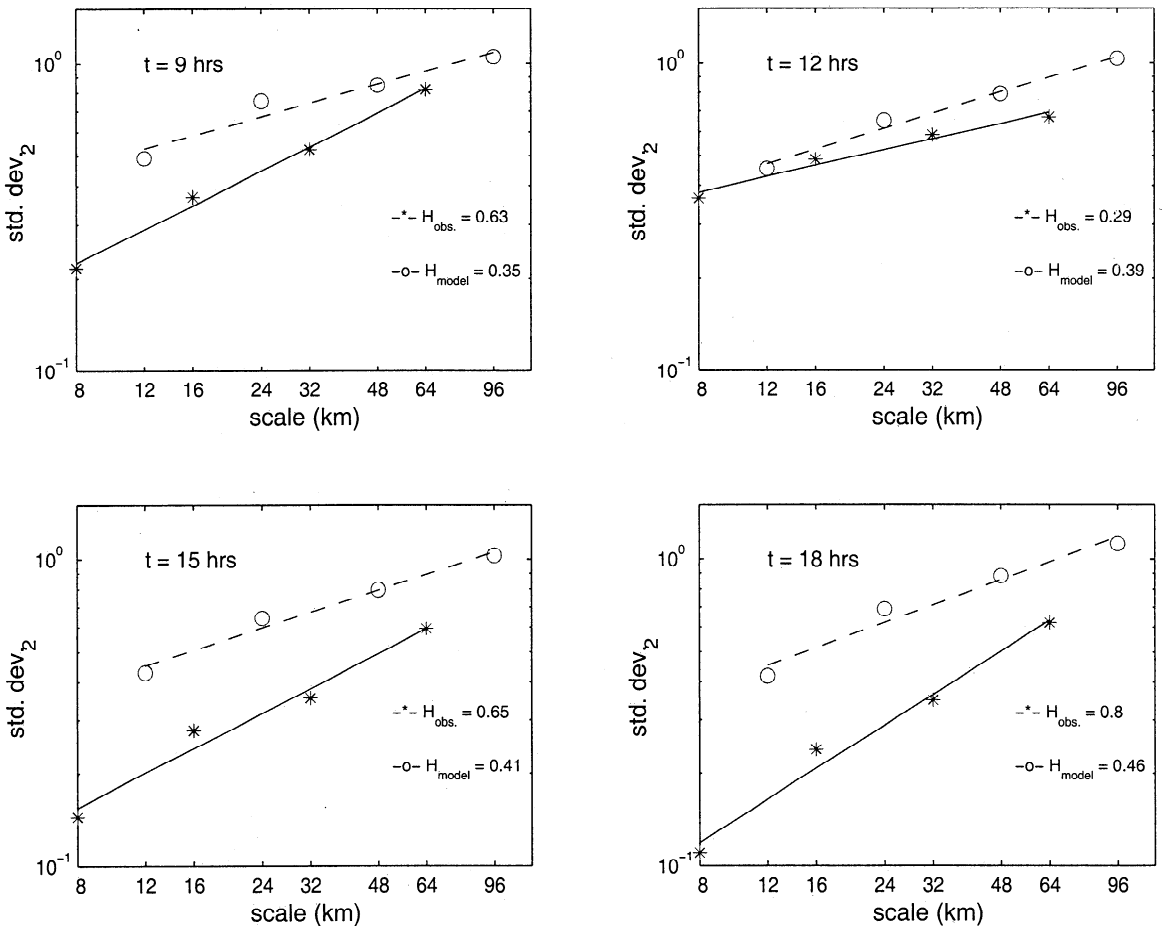

Figure 8. Standard deviations of the longitudinal normalized spatial rainfall fluctuations versus scale in a log-log plot. The plots are for 2100 UTC (top left) May 7 1995 and 0000 UTC (top right), 0300 UTC (bottom left), and 0600 UTC (bottom right) May 8 1995 for the 18-min radar-observed rainfall accumulations (stars with solid lines) and 15-min model-predicted rainfall accumulations (circles with broken lines). Log-log linearity suggests presence of simple scaling.

variation of the scaling parameters is an inherent property of the observations and confirms some distinct differences in the statistical structure of the observed and model-predicted patterns.

3.4. Spatiotemporal Organization

The radar-observed and model-predicted rainfall accumulations were analyzed for the presence of dynamic scaling. The differences in the log intensities $\Delta \ln I$ were used to characterize the evolution of the precipitation fields. Figure 11 shows the standard deviation and the mean of $\Delta \ln I$ for spatial scale $L = 4$ km and temporal scale $t = 6$ min for the observed patterns and $L = 6$ km, $t = 15$ min for the modeled patterns. The following observations can be made: (1) the mean of $\Delta \ln I$ for the observed patterns fluctuates around zero, while for the modeled patterns, it is always above zero (except for two instants of time); (2) the relative change of the standard deviation of $\Delta \ln I$ within the storm duration is larger in the observed than in the predicted patterns. *Venugopal* [1999a] analyzed several storms in different regions of the world and found that the mean of $\Delta \ln I$ always fluctuated around zero. The observed storm agrees with the findings of Venugopal, but the modeled storm does not.

To perform a dynamic scaling analysis for both the observed and predicted patterns, a period of time must be selected over which the moments of $\Delta \ln I$, $\mu(\Delta \ln I)$, and $\sigma(\Delta \ln I)$, do not vary significantly over time as compared to their average values for that period. Figure 11 shows that no such period can be found that is concurrent in both the observed and predicted patterns. Periods with small relative deviations from the average value in $\sigma(\Delta \ln I)$ had larger relative deviations in $\mu(\Delta \ln I)$ and vice versa. Thus two distinct and nonconcurrent regions in each of the observed and predicted patterns were selected: one before the transition and the other after the transition time of $t = 13$ hours. Regions 1 (duration of 3 hours) and 2 (duration of 2 hours) of the observed patterns had small relative fluctuations in both $\mu(\Delta \ln I)$ and $\sigma(\Delta \ln I)$ and were before and after the transition, respectively. For the predicted storm,

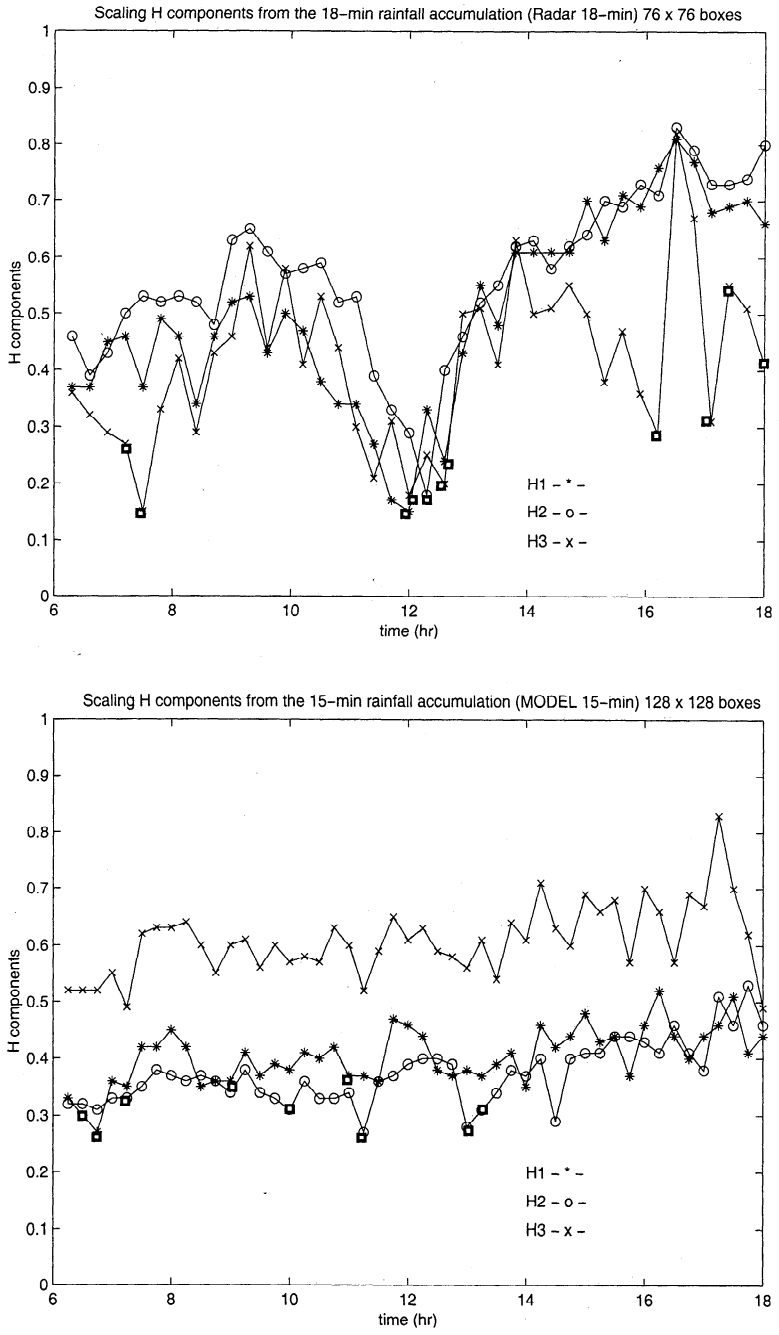

Figure 9. Scaling parameters H_1, H_2, and H_3 versus time from the (top) 18-min observed and (bottom) 15-min predicted rainfall accumulation patterns. Dark squares indicate the lack of scaling in normalized fluctuations.

Regions 1 (duration of 5 hours) and 2 (duration of 3.5 hours) were selected for similar reasons. The duration of these regions for the predicted storm was selected larger than that for the observed storm since model output was available every 15 min (instead of the 6 min for the observations), and a smaller duration would not provide enough time lags for dynamic scaling analysis.

For these regions, the pdfs of $\Delta \ln I$ were calculated for spatial scales $L = 4$, 8, 16, and 32 km and temporal scales $t = 6$, 12, 18, 24, 30, 36, 42, 48, 54, and 60 min for the observed patterns. For the model-predicted patterns the pdfs were calculated for spatial scales $L = 6$, 12, 24, and 48 km and temporal scales $t = 15$, 30, 45, 60, 75, and 90 min. Then the standard deviations $\sigma(\Delta \ln I)(L, t)$ were computed and tabulated as a function of scale L and time t. Four such tables were formed: one for each of Regions 1 and 2 of the observed fields and Regions 1 and 2 of the model-predicted fields (e.g., see Table 2 for Region 2 of the observed fields). Then, in each table, a value of $\sigma(\Delta \ln I)$ was chosen such that it

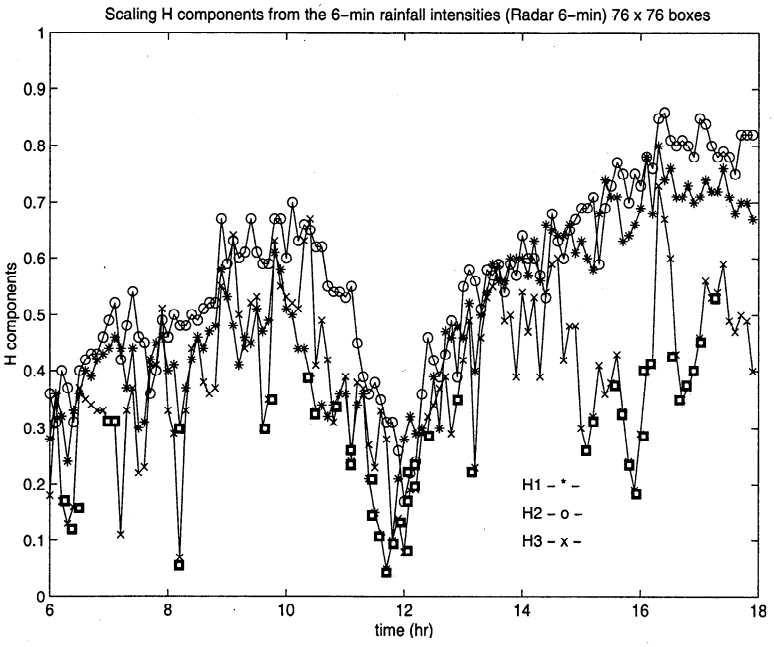

Figure 10. Scaling parameters H_1, H_2, and H_3 versus time from the 6-min radar-observed precipitation patterns. Dark squares indicate the lack of scaling in normalized fluctuations.

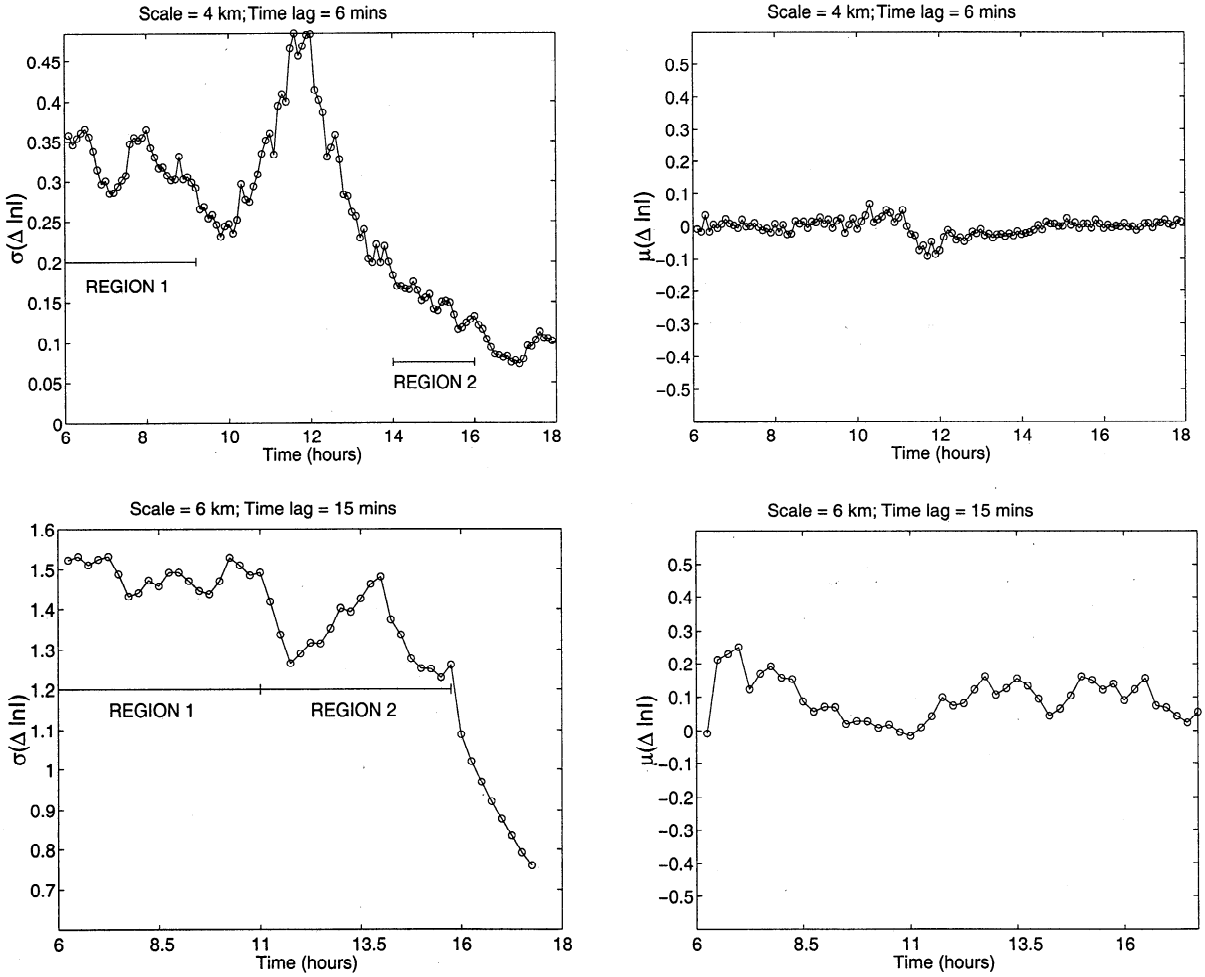

Figure 11. Standard deviation and mean of $\Delta \ln I$ for the (top) observed and (bottom) predicted patterns of the May 7-8, 1995, storm. Regions 1 and 2 are the regions over which the dynamic scaling analysis was applied.

Table 2. Standard Deviations of $\Delta \mathrm{Ln}I$ With Time Lag and Spatial Scale, for Region 2 of the Observed Patterns of the Storm of May 7-8, 1995, Over Central Oklahoma

L, km	Time Lag t, min							
	6	12	18	24	30	36	42	48
4	0.15	0.20	0.24	0.28	0.30	0.33	0.35	0.36
8	0.11	0.16	0.19	0.23	0.26	0.28	0.30	0.31
16	0.07	0.11	0.15	0.17	0.20	0.22	0.24	0.25
32	0.04	0.07	0.10	0.12	0.15	0.16	0.18	0.20

was within the range of $\sigma(\Delta \ \mathrm{ln}I)$ values of the table at each spatial scale L (e.g., the value of 0.2 in Table 2). For each spatial scale L the value of the time lag t that resulted in the chosen value of $\sigma(\Delta \ \mathrm{ln}I)$ was computed by linear interpolation. This procedure gave four pairs of (L, t) for which $\sigma(\Delta \ \mathrm{ln}I)$ was constant. These values, L, t, were plotted in a log-log plot (e.g., see bottom left plot in Figure 12 for Region 2 of the observed fields). The same procedure was applied to the other regions of the observed and model-predicted fields.

It was observed that to a good approximation, the (t, L) transformation under which the standard deviation of $\Delta \ \mathrm{ln}I$ remained constant was of the form $t/L^z =$ constant (i.e., straight line relationships on the log-log plots) for both regions and for both the observed and predicted patterns (see Figure 12). However, the values of z (estimated from the slopes of the log-log plots) were significantly different before the transition ($z = 1.4$ for the observed patterns and $z = 1.0$ for the predicted patterns) but very close to each other after the transition ($z = 0.68$ for the observed patterns and $z = 0.76$ for the predicted patterns).

To understand the significance of the z value, consider $L_2 = 2L_1$ in the relationship $t_1/t_2 = (L_1/L_2)^z$. For $z = 1$ (prediction), one will obtain $t_2 = 2t_1$ and for $z = 1.4$ (observations), $t_2 = 2^{1.4}t_1 \simeq 3.4t_1$. This implies that features twice as large will evolve two times slower in the predicted fields, and they will evolve approximately 3.4 times slower in the observed fields. Therefore the predicted fields seem to have a much faster decorrelation than the observed fields before the transition and slightly slower decorrelation after the transition.

4. Conclusions

The goal of this research was to investigate new methodologies for verification of quantitative precipitation forecasts. The underlying premise was that comparison of the multiscale spatial structure and dynamics of the observed and model-predicted patterns would provide new insights on the Quantitative Precipitation Forecast (QPF) verification problem and complement information provided by existing measures. The motivation for this belief was the fact that observed precipitation fields have been found to exhibit a self-similar structure in space and time, which apparently results from the physics of the atmosphere producing the storm. The question then was whether the model-predicted patterns exhibit the same statistical organization and whether discrepancies could reflect on how well the physics of the model emulated the physics of the atmosphere.

From the analysis of a multicell convective storm over Oklahoma, the May 7-8, 1995, storm, as observed by the Oklahoma Twin Lakes radar and as predicted by a state-of-the-art numerical weather prediction model, the following conclusions were reached:

1. The hourly accumulations of the model-predicted patterns had a spatial multiscale structure similar to that of the observed hourly accumulations. Both exhibited good scaling of the standardized rainfall fluctuations over all three directions. However, the hourly accumulations of the model-predicted patterns indicated less temporal variability of the scaling parameters H as the storm evolved while the observed hourly patterns had a much more pronounced variability of H during its evolution. Also, $H_{1,2,\mathrm{model}}$ was less than $H_{1,2,\mathrm{obs}}$ by about 0.1, although $H_{3,\mathrm{model}}$ was approximately equal to $H_{3,\mathrm{obs}}$. These findings imply that the growth of variance of the longitudinal and latitudinal standardized rainfall fluctuations as the scale increases is less in the model than in the observations. Also, the growth of variance of standardized rainfall fluctuations with scale in the diagonal component was much larger compared to the other two components in the model (by approximately 0.2). This difference was not as pronounced in the observations (see Figure 7). More analysis is needed to test whether this is simply a model artifact or signifies a real shortcoming of the model to depict the directional multiscale statistical structure of the observed fields.

2. The 15-min model-predicted rainfall accumulation

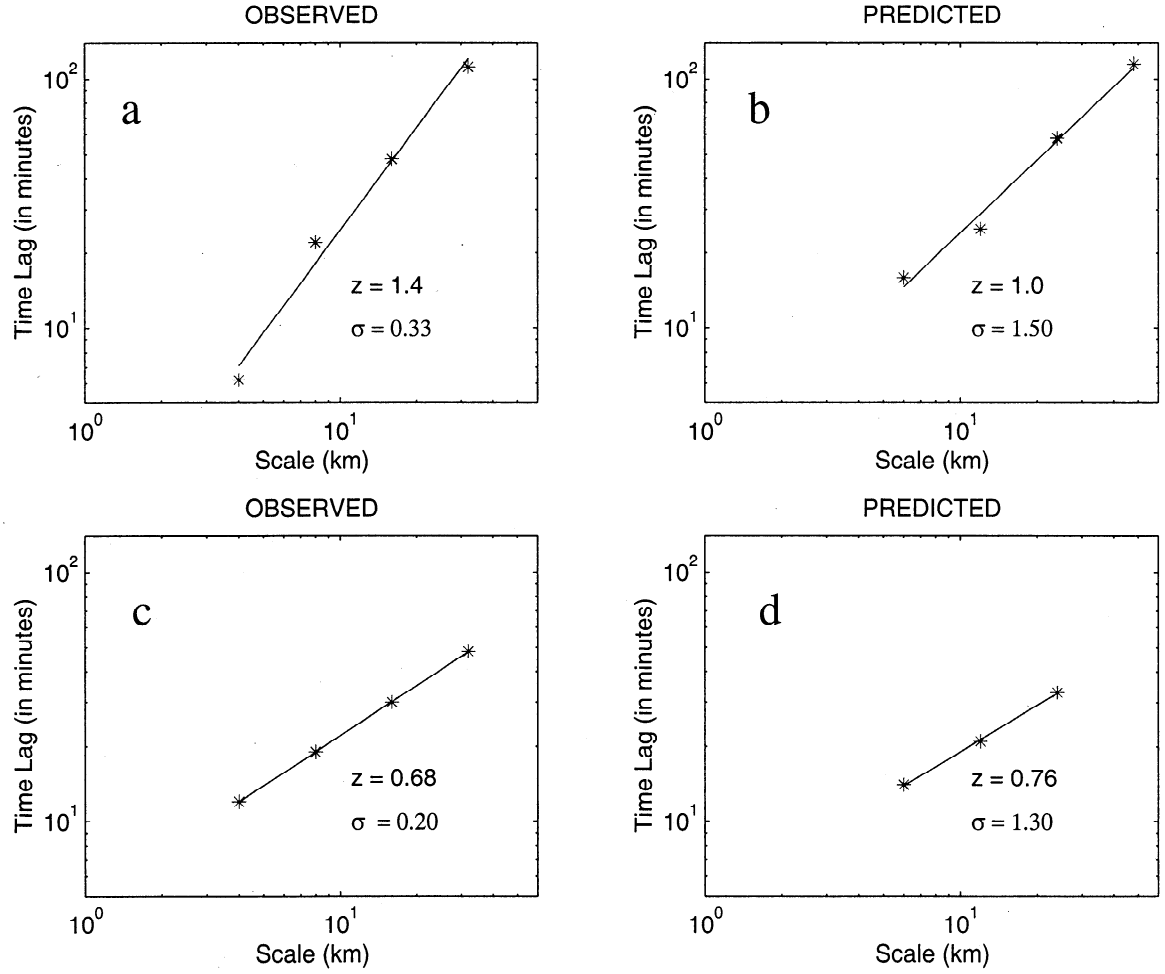

Figure 12. Dynamic scaling in the observed and predicted patterns for (a and b) Region 1 of the observed and predicted fields before the transition time of $t = 13$ hours and for (c and d) Region 2 of the observed and predicted fields after the transition time of $t = 13$ hours (see Figure 11 for the regions). The values of the estimated dynamic scaling exponent z and the constant value of $\sigma \equiv \sigma(\Delta \ln I)$ are given in each plot.

patterns compared to the 18-min observed ones revealed more distinctly some differences in the statistical structures of the observed and predicted fields. The model did not seem able to emulate the pronounced variation of the statistical structure of the observed patterns over time and produced a much smoother variation of H over the storm evolution. Consistently with the hourly comparisons, it was found that $H_{1,2,\text{model}} \leq H_{1,2,\text{obs}}$ and $H_{3,\text{model}} >> H_{1,2,\text{model}}$ (by approximately 0.2). However, for the 18-min observed accumulations, it was found that $H_{3,\text{obs}} < H_{1,2,\text{obs}}$ which was not the case for the hourly accumulations (see Figure 9). This implies that the kinetics of the storm were such that when the moving patterns were accumulated every hour, the directionality (due to the elongation of the smaller cells) was removed. Also, the scaling was not always present in the third component in the observations and scaling broke when abrupt changes in the spatial patterns occurred. The model-predicted patterns did not seem to be able to reproduce the scaling break and the pronounced temporal variability of H.

3. The standardized rainfall fluctuations in the model-predicted patterns seem to have more variability (larger σ_ξ) than in the observations. Despite the larger variability (in magnitude) of the standardized rainfall fluctuations in the model, the growth of this variability with scale (i.e., slope of the log-log linear plot of σ_ξ versus H) is smaller in the model than in the observations, at all temporal aggregation levels.

4. From the dynamic scaling analysis of the observed and predicted patterns it was found that the predicted fields had a lower dynamic scaling exponent z and thus faster temporal decorrelation than the observed fields before the transition period and a slightly slower decorrelation after the transition period. This finding coupled with a visual comparison of the observed and modeled spatial rainfall patterns suggests some inability of the model to mimic the spatiotemporal dynamics and multiscale organization of the observed patterns.

Finally, our main conclusion is that indeed multiscale measures of forecast performance are informative measures which in addition to traditional single-scale mea-

sures can provide valuable insight and quantitative assessment of not only the model's predictive ability but also about the need for improvements. Analysis of more storms is needed to conclusively establish our findings and make more general statements about the ability of numerical weather prediction models to capture the statistical structure of the observed storms. Also, analysis of the same storm predicted at higher spatial resolution (e.g., 1 or 3 km) or with different physics and more enhanced data assimilation is needed in order to understand how the proposed measures can depict small-scale differences resulting from these improvements. Such understanding will enable us to address the practical problem of pinpointing which specific improvements in model physics, data assimilation, etc. are needed on the basis of the quantified deviations of the statistical structure of observed and predicted fields. It is believed that studies of this sort can provide the means to systematically address the still open question of how the physics of the atmosphere relate to the statistics of the produced rainfall fields and how this knowledge can be used to further improve quantitative precipitation forecasting.

Acknowledgments. The material presented in this paper is based upon work jointly supported by the National Science Foundation and the National Oceanic and Atmospheric Administration under the U.S. Weather Research Program, Grant ATM-9714387. Also, partial support by the GCIP NOAA/NASA Grant NAG8-1519 and NASA TRMM Grant NAG5-7715 is greatfully acknowledged. The first author wishes to acknowledge the support of a Fellowship by the National University of Mexico. The third author was also supported under Grant ATM91-20009 to the Center for Analysis and Prediction of Storms (CAPS) at the University of Oklahoma. The authors are thankful to Venugopal Vuruputur who helped with the dynamic scaling analysis of the observed and predicted patterns and Ming Xue, Donghai Wang, and Dingchen Hou of CAPS for providing simulation output for the squall line. The atmospheric simulations were performed on the Environmental Computing Applications System (ECAS) Cray J90 at the University of Oklahoma. The ECAS is supported by NSF under Grant EAR95-12145 and by the University of Oklahoma. Statistical analysies were performed at the Minnesota Supercomputer Institute (MSI) at the University of Minnesota.

References

Benjamin, S. G., et al., The Rapid Update Cycle at NMC, Preprints, *10th Conference on Weather and Forecasting, Portland, OR*, pp. 566-568, Am. Meteorol. Soc., Boston, Mass., 1994.

Brewster, K., Application of a Bratseth analysis including Doppler radar data, *Preprints, 15th Conference on Weather and Forecasting, Norfolk, VA*, pp. 92-95, Am. Meteorol. Soc., Boston, Mass., 1996.

Droegemeier, K. K., The numerical prediction of thunderstorms: Challenges, potential benefits, and results from real time operational tests, *WMO Bull. 46*, pp. 324-336, World Meteorol. Org., Geneva, 1997.

Droegemeier, K. K., et al., Real time numerical prediction of storm-scale weather during VORTEX '95, Part I, Goals and methodology, Preprints, *18th Conference on Severe Local Storms, San Francisco, CA*, pp. 6-10, Am. Meteorol. Soc., Boston, Mass., 1996a.

Droegemeier, K. K., et al., The 1996 CAPS spring operational forecasting period - Real time storm-scale NWP, Part I, Goals and methodology, Preprints, *11th Conference on Numerical Weather Prediction, Norfolk, VA*, pp. 294-296, Am. Meteorol. Soc., Boston, Mass., 1996b.

Fritsch, J. M., et al., Quantitative precipitation forecasting: Report of the eight prospectus development team, U.S. Weather Research Program, *Bull. Am. Meteorol. Soc., 79*, 285-299, 1998.

Gupta, V. K., and E. Waymire, Multiscaling properties of spatial rainfall and river flow distributions, *J. Geophys. Res., 95*(D3), 1999-2009, 1990.

Harris, D., M. Menadbe, A. Seed, and G. Austin, Multifractal characterization of rain fields with a strong orographic influence, *J. Geophys. Res., 101*(D21), 26405-26414, 1996.

Kumar, P., and E. Foufoula-Georgiou, A multicomponent decomposition of spatial rainfall fields, 1, Segregation of large and small-scale features using wavelet transforms, *Water Resour. Res., 29*(8), 2515-2532, 1993a.

Kumar, P., and E. Foufoula-Georgiou, A multicomponent decomposition of spatial rainfall fields, 2, Self-similarity in fluctuations, *Water Resour. Res., 29*(8), 2533-2544, 1993b.

Mesinger, F., Improvements in quantitative precipitation forecasts with the Eta regional model at the National Centers for Environmental Prediction: The 48-km upgrade, *Bull. Am. Meteorol. Soc., 77*, 2637-2649, 1996.

Murphy, A. H., and R. L. Winkler, A general framework for forecast verification, *Am. Meteorol. Soc., 115*, 1330-1338, 1987.

Olsson, J., J. Niemczynowicz, and R. Berndtsson, Fractal analysis of high-resolution rainfall time series, *J. Geophys. Res., 98*(D12), 23265-23274, 1993.

Over, T. M., and V. K. Gupta, A space-time theory of mesoscale rainfall using random cascades, *J. Geophys. Res., 101*(D21), 26319-26331, 1996.

Perica, S., and E. Foufoula-Georgiou, Linkage of scaling and thermodynamic parameters of rainfall: Results from midlatitude mesoscale convective systems, *J. Geophys. Res., 101*(D3), 7431-7448, 1996a.

Perica, S., and E. Foufoula-Georgiou, A model for multiscale disaggregation of spatial rainfall based on coupling meteorological and scaling descriptions, *J. Geophys. Res., 101*(D21), 26347-26361, 1996b.

Schertzer, D., and S. Lovejoy, Physical modeling and analysis of rain and clouds by anisotropic scaling multiplicative processes, *J. Geophys. Res., 92*(D8), 9693-9714, 1987.

Shapiro, A., Z. Limin, S. Weygandt, K. Brewster, S. Lazarus, and K. Droegemeier, Initial forecast fields created from single-Doppler wind retrieval, thermodynamic retrieval and ADAS, Preprint, *11th Conference on Numerical Weather Prediction, Norfolk, VA*, pp. 5A.7-7A.7, Am. Meteorol. Soc., Boston, Mass., 1996.

Smith, J. A., D. J. Seo, M. L. Baeck, and M. D. Hudlow, An intercomparison study of NEXRAD precipitation estimates, *Water Resour. Res., 32*(7), 2035-2045, 1996.

Tessier, Y., S. Lovejoy, and D. Schertzer, Universal multifractals: Theory and observations for rain and clouds, *J. Appl. Meteorol., 32*(2), 223, 1993.

Teweles, S., and H. Wobus, Verification of prognostic charts, *Bull. Am. Meteorol. Soc., 35*, 455-463, 1954.

Veneziano, D., R. L. Bras, and J.D. Niemann, Nonlinearity and self-similarity of rainfall in time and a stochastic model, *J. Geophys. Res., 101*(D21), 26371-26392, 1996.

Venugopal, V., Spatio-Temporal organization and space-time downscaling of precipitation fields, Ph.D. thesis, Univ. of Minnesota, Minneapolis, 1999.

Venugopal, V., E. Foufoula-Georgiou, and V. Sapozhnikov, Evidence of dynamic scaling in space-time rainfall, *J. Geophys. Res.*, in press, 1999a.

Venugopal, V., E. Foufoula-Georgiou, and V. Sapozhnikov, A space-time downscaling model for rainfall, *J. Geophys. Res.*, *104*(D16), 19705-19721, 1999b.

Wang, D., M. Xue, V. Wong, and K. K. Droegemeier, Prediction and simulation of convective storms during VORTEX '95, Preprints, *11th Conference on Numerical Weather Prediction, Norfolk, VA*, pp. 10A.3-12A.3, Am. Meteorol. Soc., Boston, Mass., 1996.

Wilks, D. S., Statistical Methods in the Atmospheric Sciences: An Introduction, 464 pp., Academic Press, San Diego, Calif., 1995.

Xue, M., K. K. Droegemeier, V. Wong, A. Shapiro, and K. Brewster, *ARPS Version 4.0 User's Guide*, 380pp., Cent. for Anal. and Predict. of Storms, Norman, OK, 1995.

Xue, M., et al., Real time numerical prediction of storm-scale weather during VORTEX '95, Part II, Operations summary and example predictions, Preprints, *18th Conference on Severe Local Storms, San Francisco, CA*, pp. 178-182, Am. Meteorol. Soc., Boston, Mass., 1996a.

Xue, M., K. Brewster, K. K. Droegemeier, V. Wong, F. Carr, A. Shapiro, S. Weygandt, D. Andra, and P. Janish, The 1996 CAPS spring operational forecasting period - Real time storm-scale NWP, Part II, Operations summary and example predictions, Preprints, *11th Conference on Numerical Weather Prediction, Norfolk, VA*, pp. 297-300, Am. Meteorol. Soc., Boston, Mass., 1996b.

Zepeda-Arce, J., Multiscale statistical measures for assessment of quantitative precipitation forecasts, M.S. Thesis, Univ. of Minnesota, Minneapolis, 1999.

K. K. Droegemeier, Center for Analysis and Prediction of Storms and, School of Meteorology, University of Oklahoma, Norman, OK 73019

E. Foufoula-Georgiou and J. Zepeda-Arce, St. Anthony Falls Laboratory, Department of Civil Engineering, University of Minnesota, Minneapolis, MN 55414. (e-mail: efi@tc.umn.edu; zepe0002@tc.umn.edu)

(Received June 25, 1999; revised October 4,1999; accepted October 12,1999.)